Exploratory Study of ^{99m}Tc-EC20 Imaging for Identifying Patients with Folate Receptor–Positive Solid Tumors

Ronald E. Fisher[1], Barry A. Siegel[2], Steven L. Edell[3], Nelson M. Oyesiku[4], David E. Morgenstern[5], Richard A. Messmann[5], and Robert J. Amato[6]

[1]Methodist Hospital, Baylor College of Medicine, Houston, Texas; [2]Mallinckrodt Institute of Radiology and Siteman Cancer Center, Washington University School of Medicine, St. Louis, Missouri; [3]Delaware SPECT Imaging Center, Newark, Delaware; [4]Department of Neurosurgery, Emory University, Atlanta, Georgia; [5]Endocyte Inc., West Lafayette, Indiana; and [6]Genitourinary Oncology Program, Methodist Hospital Research Institute, Houston, Texas

^{99m}Tc-EC20 is a folate receptor (FR)–targeted imaging agent consisting of the vitamin folate conjugated to ^{99m}Tc. FR is expressed on a variety of epithelial cancers, with advanced cancers often expressing FR at significantly higher levels than earlier stages of the disease. The goals of this pilot study were to determine the percentages of various solid tumors that accumulate ^{99m}Tc-EC20 in vivo and to correlate ^{99m}Tc-EC20 uptake with immunohistochemistry (IHC) analysis of FR expression in available biopsied tumor tissue. **Methods:** A total of 154 patients with proven or suspected cancer and at least one lesion of ≥1.5 cm underwent imaging with ^{99m}Tc-EC20. The majority of these patients (77%) had a diagnosis of renal cell carcinoma. The remaining patients had a variety of other solid tumors. Whole-body planar images were obtained 1–2 h after injection, followed by SPECT of the region containing index lesions. The uptake of ^{99m}Tc-EC20 in tumors was scored as no uptake, mild uptake, or marked uptake. The resultant ^{99m}Tc-EC20 data were analyzed for correlation with the expression of the α-isoform of FR, as determined by IHC analysis, in tissue available from prior or subsequent surgery or biopsy. **Results:** The administration of ^{99m}Tc-EC20 was well tolerated. Tumors with increased ^{99m}Tc-EC20 uptake were identified in 68% of patients, and IHC results were positive for the expression of the α-isoform of FR in 67% of patients. The agreement between methods was 61% overall (κ = 0.096; 95% confidence interval = −0.085 to 0.277), with 72% agreement of positive results and 38% agreement of negative results. **Conclusion:** In vivo imaging with ^{99m}Tc-EC20 identified approximately two thirds of patients as having FR-positive tumors. Agreement between imaging and in vitro IHC was poor but was potentially confounded by a lack of correlation between the time of tissue sampling and the time of ^{99m}Tc-EC20 imaging, the heterogeneous expression of FR in metastatic lesions from the same patient, and the inability to detect the β-isoform of FR by IHC. This pilot study of ^{99m}Tc-EC20 scintigraphy indicates that the agent is safe and well tolerated and that this noninvasive procedure may have utility in selecting patients likely to benefit from FR-targeted therapy.

Received Nov. 30, 2007; revision accepted Feb. 28, 2008.

For correspondence or reprints contact: Ronald E. Fisher, Methodist Hospital, 6565 Fannin, Houston, TX 77030.

E-mail: rfisher@bcm.tmc.edu

Key Words: folate receptor; solid tumors; diagnostic imaging agent; tumor imaging; ^{99m}Tc

J Nucl Med 2008; 49:899–906
DOI: 10.2967/jnumed.107.049478

Folate transfers one-carbon chemical units from donor to acceptor molecules in a variety of biosynthetic processes (*1*), including the synthesis of nucleotide precursors of DNA. In cellular metabolism, the proliferative or kinetic state of the cell influences the rate of internalization of folate, indicating that it is critical to rapidly dividing cells, including many cancers.

Before facilitating any bioprocess, however, folate must gain entry into the cell, and in mammalian cells, entry proceeds via 2 distinct transport systems: the reduced folate carrier system, which is the primary method of folate entry into normal cells, and the folate receptor (FR) system. Although it has been noted that the FR glycoprotein is expressed in a minority of normal tissues, it is expressed at high levels on the surface of some epithelial tumors, such as ovarian cancer (*2*).

Studies evaluating over 8,000 tissue samples have shown that FR is overexpressed in cancers of the ovaries (>95% of samples tested exhibited FR expression at least 6 times greater than normal expression levels), mesothelium (≈100%), lungs (>75%), kidneys (≈65%), endometrium (≈60%), breasts (>60%), and cerebrum (≈50%) and clinically nonfunctional pituitary adenomas (~80%). It has been hypothesized that the proliferative or metabolic state of malignant cell types causes the upregulation of FR to facilitate the entry of folate for accelerated synthetic and metabolic processes (*3–15*).

The overexpression of FR on tumor cells relative to that on normal cells provides a potential mechanism for targeted antitumor therapy (*16*). Various FR-targeted therapies intended to deliver potent cytotoxic antitumor agents to cells

that selectively express FR are currently under development (*17–19*).

An important adjunct to the development of molecularly targeted therapies, including FR-targeted therapy, is the codevelopment of diagnostic tests to provide information on the presence or absence of the molecular target in question. Such diagnostic tests would allow for the "preselection" of individuals who might benefit from FR-targeted treatment and would likely play a critical role in the design and implementation of therapeutic trials. EC20 is a ^{99m}Tc-based folate-linked radiopharmaceutical that has been developed to identify patients whose tumors express FR. ^{99m}Tc-EC20 has the potential to provide the noninvasive detection of tissues expressing FR. ^{99m}Tc-EC20 targets FR with a mechanism that is identical to that used for targeting experimental therapeutic molecules (such as EC145 and EC0225) to the receptor.

The uptake of ^{99m}Tc-EC20 into solid tumors was assessed in a series of single-arm, open-label pilot studies to determine the percentages of patients whose tumors would show ^{99m}Tc-EC20 uptake; to determine the correlation of ^{99m}Tc-EC20 imaging results with the results of immunohistochemical (IHC) staining of tumor tissue for FR; and to provide information on the safety of a single injection of ^{99m}Tc-EC20 in patients with solid tumors.

MATERIALS AND METHODS

Patients

Eligible patients were at least 18 y of age and had known or suspected metastatic renal cell carcinoma (protocols EC20.3 and EC20.9), pituitary adenoma (protocol EC20.7), solid tumors (protocol EC20.8), or ovarian carcinoma or recurrent endometrial carcinoma (protocol EC20.4). Patients with at least one identifiable lesion of ≥1.5 cm, as diagnosed by CT, MRI, or ultrasonography, and good renal function (serum creatinine level ≤1.5 times the upper limit of the normal range) were enrolled in the study. Patients were asked to provide a formalin-fixed, paraffin-embedded tissue sample of the primary tumor or site(s) of metastatic or recurrent disease obtained by a previous surgical or biopsy procedure for the purpose of an IHC assay of FR (α-isoform) or were asked to provide tissue obtained at surgery or biopsy scheduled after ^{99m}Tc-EC20 imaging.

Patients were excluded from the study if they were participating simultaneously in the study of other investigational agents, had received an investigational agent or therapeutic chemotherapy within 7 d of enrollment in this trial, were unable to tolerate the conditions for radionuclide imaging, or had received another radiopharmaceutical that would have interfered with the assessment of ^{99m}Tc-EC20 distribution. Pregnant or breast-feeding women were also excluded from the study. The study protocol was approved by the institutional review board at each participating study center, and all patients gave written informed consent before participation.

Radiopharmaceutical Preparation

EC20 for injection was packaged as a sterile lyophilized powder in a single reagent vial containing the components EC20 (100 μg), sodium α-D-glucoheptonate dihydrate (80 mg), and tin(II) chloride dihydrate (80 μg). ^{99m}Tc-EC20 was prepared by adding up to 1,850 MBq of ^{99m}Tc-sodium pertechnetate into the vial and heating the vial in a boiling water bath for 18 ± 2 (mean ± SD) min. The radiochemical purity of ^{99m}Tc-EC20 was determined by thin-layer chromatography (*20*) at the time of preparation and was required to be ≥90% for administration.

Imaging Procedure

Tracer dose and imaging time were chosen in part on the basis of previous studies of ^{99m}Tc-EC20 in humans (*21*). Pharmacokinetic studies showed that the disappearance of decay-corrected radioactivity from blood fits a 2-compartment model, with harmonic means of 25 min and 29 h. These data likely reflect rapid serum clearance and urinary excretion but slow movement of the tracer from a peripheral compartment back to the blood. On the basis of human biodistribution data, radiation dosimetry with ^{99m}Tc-EC20 is comparable to that with other diagnostic radiopharmaceuticals, with an average effective dose of 1.1 mrem/MBq and the largest absorbed dose of 9.2 mrem/MBq (to the kidneys).

Patients were instructed to discontinue taking folic acid supplements for at least 2 d before their scheduled imaging study. On the day of the imaging study, patients were administered 2 intravenous injections: 1 mg of folic acid (to reduce the uptake of ^{99m}Tc-EC20 in normal tissues) and, 1–3 min later, 0.1 mg of EC20 labeled with 555–925 MBq of ^{99m}Tc-pertechnetate over 30 s in a total injection volume of 1–2 mL. Each injection was given as a slow intravenous push via a free-flowing indwelling intravenous catheter in an upper-extremity vein (i.e., in the antecubital fossa). The mean administered activity was 851 MBq (range, 606.8–1,054.5 MBq). The mean activity injected per kilogram of body weight was 10.73 MBq (range, 4.81–19.98 MBq/kg).

At approximately 1–2 h after injection, anterior and posterior midthigh to head planar images were acquired in a 256 × 1,024 (minimum) matrix word-mode format with a total scan time of 20–35 min. The images were obtained with a dual-detector, large–field-of-view γ-camera that was equipped with low-energy, high-resolution parallel-hole collimators. A 20% symmetric energy window was centered over the 140-keV photopeak of ^{99m}Tc.

SPECT images of the region that was known to contain the target lesion(s), as identified by conventional imaging (CT, MRI, or ultrasonography), were obtained after planar imaging. The SPECT images included 120–128 total projections over 360° with 15–20 s per stop and were reconstructed in 3 orthogonal planes.

Image Interpretation

An on-site nuclear medicine physician, who was unaware of the outcome of the IHC assay, evaluated the planar and SPECT images for the uptake of ^{99m}Tc-EC20 in the identified lesions. The physician used the conventional imaging studies to identify up to 3 presumed malignant lesions of ≥1.5 cm (one dimension) for each patient and compared the uptake of ^{99m}Tc-EC20 in these lesions with the background. The uptake of ^{99m}Tc-EC20 in the lesions was scored as no uptake (less than or equal to background), mild uptake (slightly increased compared with background), or marked uptake (strikingly increased compared with background). A result of "no uptake" was scored as ^{99m}Tc-EC20 negative, whereas a result of "mild uptake" or "marked uptake" was scored as ^{99m}Tc-EC20 positive (EC20+). On the basis of the expected uptake observed in animal models and a phase I dosimetry study, the uptake of ^{99m}Tc-EC20 in the kidneys, liver, bladder, and spleen was assessed with the same 3-point scale as that used for

malignant lesions. Additional areas of uptake were recorded when noted by the physician.

Tissue FR Assay

The formalin-fixed, paraffin-embedded tissue samples available from surgery or biopsy were analyzed for FR by an IHC assay specific for the α-isoform of FR. Evaluation of the stained samples was accomplished in a semiquantitative manner with a light microscope to assess the degree of circumferential membranous staining in the tumor cell population. The findings were classified into 1 of 4 categories: 0 = no staining in tumor cells above background; 1+ = weak staining in ≥5% of tumor cells; 2+ = moderate staining in ≥5% of tumor cells; and 3+ = strong staining in ≥5% of tumor cells. A staining result of 0 was scored as IHC negative, whereas a staining result of 1+, 2+, or 3+ was scored as IHC positive.

Safety Assessment

Vital signs were obtained within 5 min of injection (baseline) and at 1 h after injection. Blood and urine specimens for clinical laboratories were obtained within 2 h of injection and at 22–28 h after injection. Treatment-emergent adverse events were monitored through the time of the patient's follow-up laboratory measurements at 22–28 h after injection. Additionally, the patients were instructed to report any adverse events that occurred up to 7 d after injection.

Statistical Methods

The number of patients characterized as having tumors with no uptake, mild uptake, or marked uptake of ^{99m}Tc-EC20 and the number of patients who had IHC staining results of 0, 1+, 2+, or 3+ were tabulated, and the percentage of patients who had EC20+ tumors, as determined by ^{99m}Tc-EC20 imaging (i.e., those whose tumors showed mild or marked uptake), and FR-positive (FR+) tumors, as determined by IHC staining (i.e., those who had a score of 1+, 2+, or 3+) were calculated. A 2 × 2 frequency table was constructed to compare the ^{99m}Tc-EC20 imaging and IHC staining results.

The overall percentage of agreement of the 2 methods, the agreement of positive ^{99m}Tc-EC20 imaging results and positive IHC results, and the agreement of negative ^{99m}Tc-EC20 imaging results and negative IHC results were calculated. A κ-coefficient with a 95% confidence interval (CI) was calculated to examine the agreement between the 2 methods (*22,23*).

Adverse events, clinical laboratory evaluations, and vital signs were summarized descriptively. Quantitative laboratory measurements were categorized according to the normal reference range (low, normal, and high), and shift tables of the frequencies for preinjection versus postinjection categories were prepared. Changes in laboratory values and vital signs that met predefined criteria for clinical significance were summarized.

RESULTS

Patients

A total of 155 patients were enrolled and underwent imaging with ^{99m}Tc-EC20 at 6 centers between 15 April 2003 and 31 August 2005. One patient later withdrew his consent for his scan to be included in the study and therefore was included only in the safety data presented here, not the imaging data. One patient received a second administration of ^{99m}TC-EC20 approximately 77 d after his initial imaging to assess uptake after resection of his primary tumor. This patient's data for both assessments were included in assessments of efficacy and safety but were counted only once for the determination of baseline demographics. The study population was primarily white (92%) and male (64%) and ranged in age from 32 to 80 y (mean, 57.8 y). The tumor types were primarily renal cell carcinomas (119 patients), benign ovarian tumors (8 patients), ovarian carcinomas (7 patients), breast carcinomas (6 patients), and pituitary adenomas (6 patients). The remaining 8 patients had small cell lung carcinoma; lung carcinoma (type unspecified); colon, endometrial, and thyroid carcinomas; non-Hodgkin's lymphoma; sarcoma; and glioma (1 patient each). Approximately 88% of patients had metastatic disease at the time of study entry, with the lungs (74%), lymph nodes (45%), liver (29%), and bone (23%) representing the primary sites of metastasis.

The mean time from the initial cancer diagnosis to the time of the ^{99m}Tc-EC20 scan was 45.2 mo (range, −0.8 to 221.3 mo), and the mean time from the most recent recurrence or progression to the time of the ^{99m}Tc-EC20 scan was 2.4 mo (range, −0.6 to 36.6 mo). A total of 155 patients completed the study (i.e., they received ^{99m}Tc-EC20) and had at least one scan (either planar imaging or SPECT).

Biodistribution

The percentage of patients with uptake in the liver, kidneys, bladder, spleen, and other organs are shown in Table 1. Physiologic (usually marked) uptake of ^{99m}Tc-EC20 was noted in the kidneys and bladder in almost all patients, consistent with the known expression of FR on the proximal tubules of the kidneys (*24*) and the urinary excretion of the tracer. Mild to marked uptake was also seen in the liver in all patients, causing hepatic lesions (when present) to appear as photopenic defects, even in patients with marked uptake in lesions elsewhere in the body. Hepatic uptake of ^{99m}Tc-EC20 has been seen in animal models (*20*); however, it can be partially blocked by inhibitors of organic anion transport, suggesting that it is mediated, at least in part, by mechanisms other than FR binding (C.P. Leamon, oral communication, July 2007). Uptake (usually mild) was frequently seen in the

TABLE 1
Biodistribution of ^{99m}TC-EC20

Organ or tissue	% of patients with following ^{99m}Tc-EC20 uptake: None*	Mild	Marked
Kidneys	1	9	91
Bladder	2	12	87
Liver	0	8	92
Spleen	30	57	12
Nasopharynx	NA	7	0
Choroid plexus	NA	4	0
Thyroid	NA	3	0
Stomach	NA	1	0

*Uptake in organs other than kidneys, bladder, liver, and spleen is noted only when present. NA = not applicable.

spleen and rarely in other organs not associated with the tumors, such as the thyroid, lymph nodes, bowel, stomach, and joints. Uptake in the thyroid, bowel, stomach, and choroid plexus was uncommon and likely was related to a small amount of free ^{99m}Tc-pertechnetate which was easily recognizable and had no appreciable effect on image interpretation. Spleen uptake is related to the known presence of the β-isoform of FR in normal splenic tissue, as well as the presence of FRs on activated macrophages (*25,26*). Uptake (usually mild) in bone marrow was observed in nearly all patients and was assumed to reflect the normal physiologic distribution of the tracer.

Efficacy Results

^{99m}Tc-EC20 images were evaluated for 154 patients; conventional images for the identification of target lesions were unavailable for 1 patient for comparison with the ^{99m}Tc-EC20 images. Of the 154 patients who were evaluated, 105 (68%) had at least one metastatic site that showed uptake of ^{99m}Tc-EC20 on either planar imaging or SPECT and were therefore classified as having EC20+ tumors (Table 2). Of the 105 patients who had EC20+ tumors, 57 (54%) had tumors that showed marked uptake of ^{99m}Tc-EC20 and 48 (46%) had tumors that showed mild uptake. A total of 374 lesions were evaluated by planar imaging, and 369 lesions were evaluated by SPECT. When assessed by planar imaging, 141 lesions (38%) showed ^{99m}Tc-EC20 uptake, with 66% of these showing mild uptake and 34% showing marked uptake. When assessed by SPECT, 185 lesions (50%) showed ^{99m}Tc-EC20 uptake, with 58% of these showing mild uptake and 42% showing marked uptake. Figure 1 shows representative whole-body planar scintigrams, SPECT images, and corresponding CT images that exhibit the localization of ^{99m}Tc-EC20 in a radiographically demonstrable chest wall metastasis. Figure 2 shows marked uptake in a metastasis in the paraspinal muscles. Figures 1 and 2 also demonstrate subtle uptake in other, smaller metastases.

Of the 155 patients who completed the study, 123 had samples available for IHC staining. As determined by IHC staining for the α-isoform of FR, 67% of these patients had FR+ tumors (Table 3). Overall, the ^{99m}Tc-EC20 image evaluations corresponded to the IHC staining results for 61% of the patients (Tables 4 and 5). The κ-coefficient was 0.096 (95% CI = −0.085 to 0.277), indicating poor chance-corrected agreement. The agreement of EC20+ results with FR+ results was 72%, whereas the agreement of ^{99m}Tc-EC20–negative results with FR-negative results was 38%.

Fewer than 5% of patients had metastatic disease detected by ^{99m}Tc-EC20 imaging that was not detected by CT. None of these additional sites of metastatic disease would have changed the staging of the tumors (other metastatic sites had been detected by CT).

Approximately 30% of the patients were found to have mild to moderate uptake within numerous small foci in the inguinal and axillary regions. When present, these were always multifocal and bilateral. Lymph nodes in these regions were consistently considered normal on the basis of CT criteria.

Safety Results

A total of 17 adverse events were reported in 13 (8%) of the 155 patients receiving ^{99m}Tc-EC20. Only 3 events (lower abdominal pain in 1 patient and nausea and vomiting in 1 patient) were considered by the investigator to be "possibly related" to the study treatment. Adverse events in 7 patients resulted in hospitalization and, thus, were categorized as serious adverse events. None of the serious adverse events was considered by the investigator to be "related" to the administration of ^{99m}Tc-EC20.

TABLE 2
^{99m}Tc-EC20 Image Evaluation

Tumor type	No. of patients evaluated	No. of patients with the following ^{99m}Tc-EC20 uptake*: None	Mild	Marked	Overall (%)
Benign ovarian	8	8	0	0	0
Brain	1	0	1	0	1/1 (100)
Breast	6	3	2	1	3/6 (50)
Colon	1	1	0	0	0
Endometrium	1	0	0	1	1/1 (100)
Lung	2	0	1	1	2/2 (100)
Malignant ovarian	7	3	2	2	4/7 (57)
Non-Hodgkin's lymphoma	1	0	1	0	1/1 (100)
Pituitary	7	3	1	3	4/7 (57)
Renal	118	31	39	48	87/118 (74)
Soft-tissue sarcoma	1	0	0	1	1/1 (100)
Thyroid	1	0	1	0	1/1 (100)
Overall	154	49	48	57	105 (68)

*Overall uptake represents highest intensity of uptake indicated by on-site, masked nuclear medicine physician (i.e., none, mild, or marked). Overall score for given patient was positive when at least 1 lesion had mild or marked uptake of ^{99m}Tc-EC20.

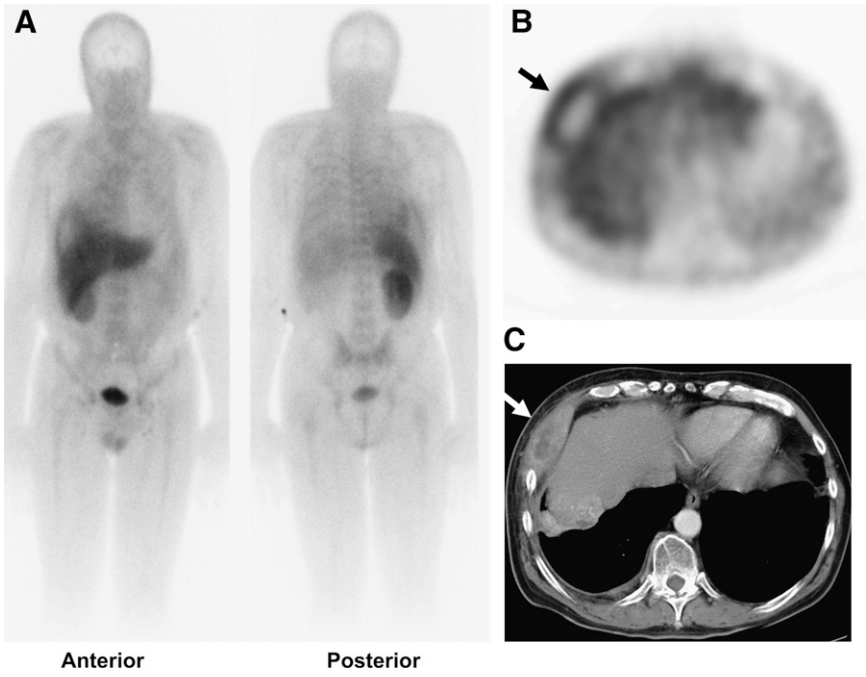

FIGURE 1. Anterior and posterior whole-body planar (A) and transverse SPECT (B) ^{99m}Tc-EC20 images in 59-y-old man with renal cell carcinoma revealed large, destructive right chest wall metastasis (arrow). Scintigraphic findings correlated well with those on CT image (C), including photopenia in area of central necrosis. These scintigraphic results suggested that lesion was FR+. Note faint uptake in left renal fossa, thought to represent postsurgical inflammation. Mild uptake in right lung and right paratracheal region corresponded to other sites of metastatic disease demonstrated on CT (not shown). Small foci of mild ^{99m}Tc-EC20 uptake were noted in inguinal regions bilaterally; this finding was seen in many patients and may be secondary to FRs on activated macrophages.

No "clinically important effects" were observed with regard to hematology, serum chemistry, or urinalysis, as judged on the basis of the mean change in values from before injection to after injection of ^{99m}Tc-EC20. No systematic shifts from normal values before injection to abnormal values after injection were observed for any laboratory test, and none of the patients had postinjection laboratory values that the investigator considered to be clinically significant. No "clinically important effects" were observed for heart rate or for systolic or diastolic blood pressure at 1 h after injection of ^{99m}Tc-EC20.

DISCUSSION

High-affinity FRs are overexpressed in several human cancers, including those of the ovaries, brain (i.e., meningiomas, ependymomas, and brain metastases), endometrium, and kidneys (*3–13*). ^{99m}Tc-EC20, an FR-targeted diagnostic agent, allows for noninvasive, whole-body assessments of FR

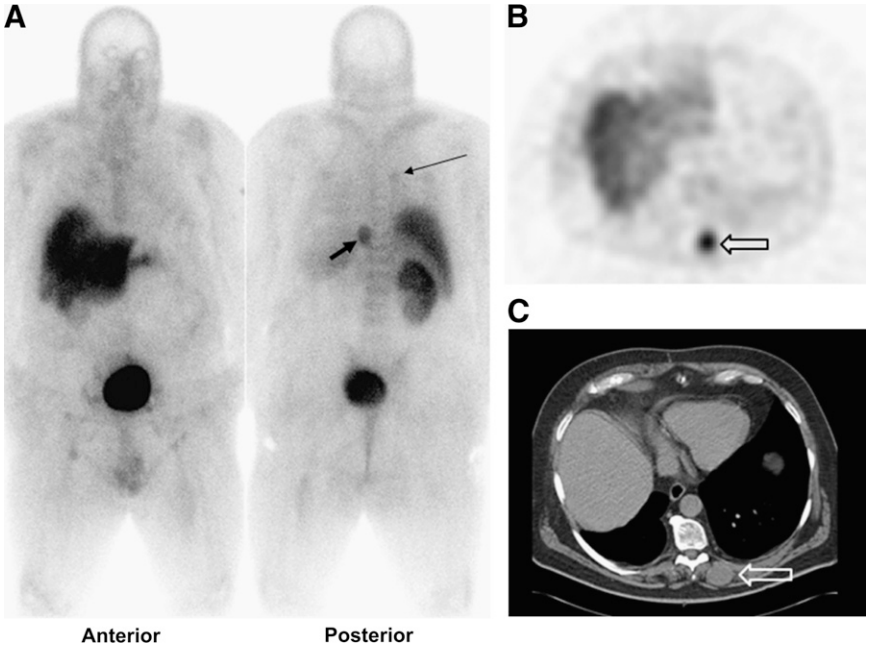

FIGURE 2. ^{99m}Tc-EC20 images of 57-y-old man with known pulmonary metastases from renal cell carcinoma. Anterior and posterior whole-body planar images (A) revealed faint uptake of tracer in right upper-lobe pulmonary nodule (1.8 × 2.1 cm) (thin arrow) that was demonstrated on CT (not shown). More intense tracer uptake was seen in mass (2.7 × 3.5 cm) (thick arrow) in left paraspinal muscles. Planar images also revealed faint bilateral inguinal nodal uptake of ^{99m}Tc-EC20. Paraspinal mass also was demonstrated on transverse SPECT image (B) and corresponding CT image (C) (arrows).

TABLE 3
Distribution of IHC Scores

Tumor type	No. of samples evaluated	No. of samples with the following score: 0	1+	2+	3+	Total no. (%) of FR+ samples
Benign ovarian	2	2	0	0	0	0
Breast	4	2	1	1	0	2/4 (50.0)
Colon	1	1	0	0	0	0
Malignant ovarian	6	0	1	3	2	6/6 (100)
Renal	109	36	46	17	10	73/109 (67.0)
Soft-tissue sarcoma	1	0	0	1	0	1/1 (100)
Overall	123	41	48	22	12	82/123 (66.7)

expression status and, thus, may identify patients who have FR+ tumors and who may benefit from FR-targeted therapy. Preclinical (animal) imaging studies have been performed with normal and M109 tumor–bearing BALB/c mice (*19,20*). These studies showed scintigraphically detectable uptake in FR+ tumors placed intraperitoneally or subcutaneously. The uptake of ^{99m}Tc-EC20, quantified by an in vitro assay, was proportional to FR density and to tumor size. Such results suggested that ^{99m}Tc-EC20 could be used to detect FR+ tumors in humans noninvasively. This report represents the first published data on the use of ^{99m}Tc-EC20 to image tumors in humans.

A single injection of ^{99m}Tc-EC20 was well tolerated. Only 8% of patients experienced an adverse event during administration and the follow-up period, and only 3 adverse events were considered to be "possibly related" to the injection. No drug-related serious adverse events occurred, and no clinically important effects of ^{99m}Tc-EC20 on laboratory assays or on the monitoring of vital signs were observed.

The results of the present study of 154 patients with a variety of solid tumors demonstrated that 68% of the patients showed uptake of ^{99m}Tc-EC20 in their tumors (i.e., EC20+ tumors). In comparison, IHC staining for the α-isoform of FR in 123 patients demonstrated that 67% of these patients had FR+ tumors. In all patients, the correlation of the ^{99m}Tc-EC20 imaging results with the IHC staining results was 61%, although there was better agreement for positive imaging and staining results than for negative imaging and staining results (72% vs. 38%). Chance-corrected agreement between ^{99m}Tc-EC20 imaging results and IHC staining results was poor ($\kappa = 0.096$; 95% CI = −0.085 to 0.277).

When considering the relatively poor agreement between the results of ^{99m}Tc-EC20 imaging and IHC, one must recognize that the present study was not designed as a lesion-to-lesion comparison of ^{99m}Tc-EC20 imaging and IHC. In most cases, the tissue samples available were limited to the primary neoplasm (often obtained months or years before study entry), and scanning was performed in patients with metastatic disease after resection of the primary neoplasm. Surgical removal or biopsy and IHC analysis of all of the metastatic lesions imaged in the present study would have been scientifically preferable but was not performed for practical and ethical reasons. Furthermore, the clinical relevance of such data is limited because of differences in the types of FRs detected by IHC and imaging, as discussed in the next paragraph.

Discrepant results for the 2 methods may reflect a difference in the FR status of the primary neoplasm versus the metastatic disease after excision of the primary tumor or heterogeneity in FR expression between metastatic lesions within a patient. In fact, evidence supporting both of these hypotheses exists. Studies comparing FR expression with tumor stage have suggested that FR expression is increased in more advanced (i.e., metastatic) disease (*11*). In the present study, 42% of patients with renal cell carcinomas had a heterogeneous mixture of lesions, including some with no

TABLE 4
Comparison of ^{99m}Tc-EC20 Imaging Results and IHC Staining Results

Investigator evaluation of ^{99m}Tc-EC20 image	IHC result: Tissue positive	Tissue negative	Total
Positive	59	25	84
Negative	23	15	38
Total	82	40	122

TABLE 5
Agreement of ^{99m}Tc-EC20 Imaging Results and IHC Staining Results

Parameter	Value
Overall agreement of ^{99m}Tc-EC20 with IHC	61% (74/122)
Agreement of ^{99m}Tc-EC20 positive with IHC positive	72% (59/82)
Agreement of ^{99m}Tc-EC20 negative with IHC negative	38% (15/40)
κ-coefficient (95% CI)	0.096 (−0.085 to 0.227)

uptake and others with mild or marked uptake. An additional consideration is that only 1 of the 2 FR isoforms (α-isoform) is detected by IHC, and IHC may detect nonfunctional as well as functional receptors. In contrast, ^{99m}Tc-EC20 is capable of recognizing and binding to both the α-isoform and the β-isoform of FR and only binds functional receptors that are accessible to the imaging agent. All of these issues suggest that ^{99m}Tc-EC20 imaging may be a more accurate means of predicting the response to FR-targeted therapy than is IHC, particularly IHC performed on the primary tumor. The ultimate test of this hypothesis will require a therapeutic clinical trial in which the response to FR-targeted therapy is correlated with ^{99m}Tc-EC20 scan results. Such a trial is already under way.

Other explanations for the lack of correlation include the possibility that uptake, particularly in larger and more destructive lesions, may have been secondary to associated inflammation, an observation consistent with the presence of FRs on the surface of activated macrophages (*26*) and the localization of ^{99m}Tc-EC20 uptake in the joints of patients with active rheumatoid arthritis (*27*). Finally, the high background activity found in the liver precluded an assessment of the FR status of hepatic metastases, as all metastases were either undetectable or photopenic.

Few previously unknown sites of metastatic disease were discovered on the scans. However, the present study was not designed to test the usefulness of ^{99m}Tc-EC20 in improving the staging of renal cell carcinomas or other cancers. The majority of patients enrolled in the present study already had known distant metastases; therefore, staging was not likely to be altered. A study addressing this topic would best be performed with patients who have lower stages of disease.

An interesting incidental finding was that of mild to moderate uptake within numerous foci in the inguinal and axillary regions bilaterally in some patients. Although the basis and clinical relevance of this uptake are uncertain, the uptake may identify lymph nodes harboring activated macrophages, known to express FRs.

CONCLUSION

A single intravenous injection of ^{99m}Tc-EC20 resulted in detectable uptake on planar scintigraphy or SPECT for 68% of patients and was well tolerated by adult patients with a variety of solid tumors. The true accuracy of scintigraphy in identifying patients with FR+ metastases and thereby successfully selecting patients for FR-directed therapy could not be assessed in the present study. The ^{99m}Tc-EC20 imaging results, which mainly assessed metastatic sites, did not correlate well with the IHC staining results. However, IHC analysis was largely limited to primary tumor samples; therefore, the lack of correlation is not surprising, given that the FR status of metastases is often different from that of the primary tumor and given the other reasons discussed earlier.

^{99m}Tc-EC20 imaging is a safe, noninvasive procedure that may identify FRs in recurrent or metastatic disease without the need for biopsy and that may have utility in identifying patients who may benefit from treatment with FR-targeted therapy.

ACKNOWLEDGMENTS

The study was supported by Endocyte, Inc. The authors gratefully acknowledge the contributions of the following investigators: Farrokh Dehdashti, Washington University, St. Louis, MO (image review); James W. Fletcher, Indiana University Hospital, Indianapolis, IN (image review); Raghuveer Halkar, Emory University, Atlanta, GA (image review); Val J. Lowe, Mayo Clinic, Rochester, MN (image review); and Joel Picus, Washington University, St. Louis, MO (patient recruitment). We also thank Sue Bever (study management), Natalie Carnahan (data management), and Sujana Santhapuram (data management) of Endocyte, Inc., for their contributions to this study and Dr. Chris Leamon for help in preparing the article.

REFERENCES

1. Scott JM, Weir DG. Folate/vitamin B12 inter-relationships. In: Tipton KF, ed. *Essays in Biochemistry.* Dublin, Ireland: Portland Press; 1994:63–72.
2. Coney LR, Tomassetti A, Carayannopoulos L, et al. Cloning of a tumor-associated antigen: MOv18 and MOv19 antibodies recognize a folate-binding protein. *Cancer Res.* 1991;51:6125–6132.
3. Ross JF, Chaudhuri PK, Ratnam M. Differential regulation of folate receptor isoforms in normal and malignant tissues in vivo and in established cell lines. *Cancer.* 1994;73:2432–2443.
4. Garin-Chesa P, Campbell I, Saigo PE, Lewis JL Jr, Old LJ, Rettig WJ. Trophoblast and ovarian cancer antigen LK26. *Am J Pathol.* 1993;142:557–567.
5. Holm J, Hansen SI, Hoier-Madsen M, Søndergaard K, Bzorek M. Folate receptor of human mammary adenocarcinoma. *APMIS.* 1994;102:413–419.
6. Holm J, Hansen SI, Hoier-Madsen M, Helkjaer PE, Bzorek M. Folate receptor in malignant effusions of ovarian carcinoma. *APMIS.* 1995;103:663–670.
7. Holm J, Hansen SI, Hoier-Madsen M, Helkjaer PE, Nichols CW. Folate receptors in malignant and benign tissues of human female genital tract. *Biosci Rep.* 1997;17:415–427.
8. Weitman SD, Lark RH, Coney LR, et al. Distribution of the folate receptor GP38 in normal and malignant cell lines and tissues. *Cancer Res.* 1992;52:3396–3401.
9. Franklin W, Waintrub M, Edwards D, et al. New anti-lung-cancer antibody cluster 12 reacts with human folate receptors present on adenocarcinoma. *Int J Cancer Suppl.* 1994;8:89–95.
10. Li PY, Del Vecchio S, Fonti R, et al. Local concentration of folate binding protein GP38 in sections of human ovarian carcinoma by in vitro quantitative autoradiography. *J Nucl Med.* 1996;37:665–672.
11. Toffli G, Cernigoi C, Russo A, Gallo A, Bagnoli M, Boiocchi M. Overexpression of folate binding protein in ovarian cancers. *Int J Cancer.* 1997;74:193–198.
12. Bueno R, Appansani K, Mercer H, Lester S, Sugarbaker D. The alpha folate receptor is highly activated in malignant pleural mesothelioma. *J Thorac Cardiovasc Surg.* 2001;121:225–233.
13. Parker N, Turk MJ, Westrick E, Lewis JD, Low PS, Leamon CP. Folate receptor expression in carcinomas and normal tissues determined by a quantitative radioligand binding assay. *Anal Biochem.* 2005;338:284–293.
14. Evans C-O, Young AN, Brown MR, et al. Novel patterns of gene expression in pituitary adenomas identified by cDNA microarrays and quantitative RT-PCR. *J Clin Endocrinol Metab.* 2001;86:3097–3107.
15. Evans C-O, Reddy P, Brat DJ, et al. Differential expression of folate receptor in pituitary adenomas. *Cancer Res.* 2003;63:4218–4224.
16. Low PS, Antony AC. Folate receptor-targeted drugs for cancer and inflammatory diseases. *Adv Drug Deliv Rev.* 2004;56:1055–1058.
17. Reddy JA, Dorton R, Westrick E, et al. Preclinical evaluation of EC145, a folate-vinca alkaloid conjugate. *Cancer Res.* 2007;67:4434–4442.
18. Sausville E, LoRusso P, Quinn M, et al. A phase I study of EC145 administered weeks 1 and 3 of a 4-week cycle in patients with refractory solid tumors [abstract]. *J Clin Oncol.* 2007;25(suppl):2557.

19. Leamon CP, Reddy JA, Vlahov IR, et al. Preclinical antitumor activity of a novel folate-targeted dual drug conjugate. *Mol Pharm.* 2007;4:659–667.
20. Reddy JA, Xu L-C, Parker N, Vetzel M, Leamon CP. Preclinical evaluation of ^{99m}Tc-EC20 for imaging folate receptor–positive tumors. *J Nucl Med.* 2004;45:857–866.
21. Endocyte, Inc. *FolateScan (^{99m}Tc-EC20) Investigator's Brochure, Version 10.0.* West Lafayette, IN: Endocyte Inc.; 2007.
22. Altman DG. *Practical Statistics for Medical Research.* New York, NY: Chapman and Hall; 1990.
23. Landis JR, Koch GG. The measurement of observer agreement for categorical data. *Biometrics.* 1977;33:159–174.
24. Selhub J, Franklin WA. The folate-binding protein of rat kidney: purification, properties, and cellular distribution. *J Biol Chem.* 1984;259:6601–6606.
25. Nakashima-Matsushita N, Homma T, Yu S, et al. Selective expression of folate receptor beta and its possible role in methotrexate transport in synovial macrophages from patients with rheumatoid arthritis. *Arthritis Rheum.* 1999;42:1609–1616.
26. Turk MJ, Bruer GJ, Widmer WR, et al. Folate-targeted imaging of activated macrophages in rats with adjuvant-induced arthritis. *Arthritis Rheum.* 2002;46: 1947–1955.
27. Matteson E, Lowe VJ, Prendergast FG, et al. Assessment of disease activity in rheumatoid arthritis using a novel folate targeted radiopharmaceutical, FolateScan [abstract]. *Arthritis Rheum.* 2007;56(suppl):S285.